Convective and Stably Stratified Turbulence and Internal Gravity Waves

Igor Rogachevskii and Nathan Kleeorin

Ben-Gurion University of the Negev, Beer-Sheva, Israel
NORDITA, KTH Royal Institute of Technology and Stockholm University, Sweden

Sergej Zilitinkevich

University of Helsinki and Finnish Meteorological Institute, Helsinki, Finland

Outline

- Introduction
- Stably stratified turbulence (SST) without waves
- Stably stratified turbulence with internal gravity waves
- Stably stratified turbulence produced by internal gravity waves
- Detection of internal gravity waves in laboratory experiments with turbulent convection
- Convective turbulence

Sources for Stably Stratified Turbulence

- External Large-Scale Shear (mean wind in atmospheric turbulence);
- Shear in large-scale circulation in convection
- Internal Gravity Waves
- Forcing in DNS, LES and laboratory experiments (oscillating grids; propellers, etc).

Budget Equation for TKE

$$\frac{\partial E_K}{\partial t} = \Pi_{tot} - T - D$$

$$E_K = \frac{1}{2}\langle \mathbf{u}^2 \rangle$$

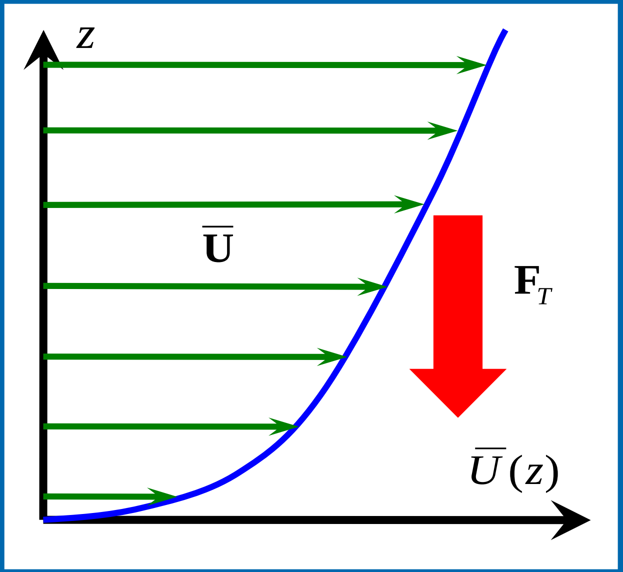

Balance in R-space

$$\Pi_{tot} \approx D$$

$$\mathbf{S} = \frac{\partial \overline{\mathbf{U}}}{\partial z}$$

$$T = \mathrm{div}\, \mathbf{\Phi}_u$$

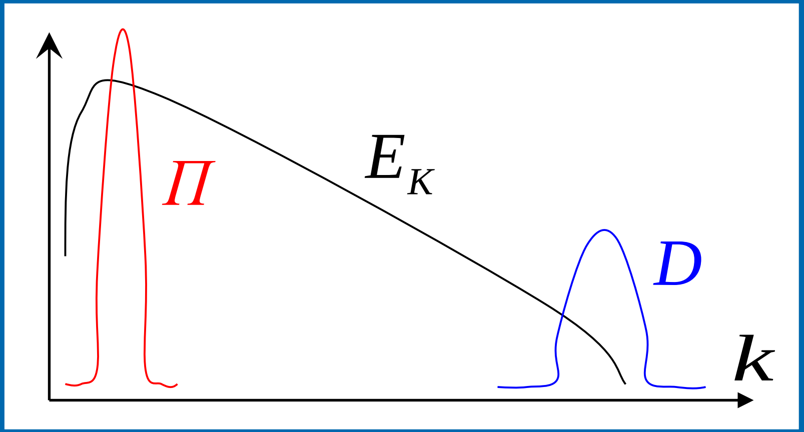

$$\frac{\partial E_K}{\partial t} = K_M S^2 - \beta |F_z| - \frac{E_K}{t_T} - T$$

$$\Pi = -\langle u_i u_j \rangle \nabla_j \bar{U}_i = K_M S^2$$

$$K_M \equiv \nu_T$$

$$\mathrm{Ri} = \frac{N^2}{S^2} \qquad N^2 = \beta \frac{\partial \overline{\Theta}}{\partial z}$$

Steady-state for homogeneous turbulence:

$$t_T = \frac{l}{\sqrt{E_K}} \qquad \boldsymbol{\beta} = \frac{\mathbf{g}}{T_0}$$

$$E_K \approx t_T (K_M S^2 - \beta |F_z|)$$

TKE Balance for Stably Stratified Turbulence

$$\frac{\partial E_K}{\partial t} = K_M S^2 - \beta \,|\, F_z \,| - \frac{E_K}{t_T} - T$$

$$\begin{tikzcd} \boxed{S} \arrow[r] & \boxed{TKE} \arrow[r] \arrow[d] & \boxed{D_K} \\ & \boxed{B} & \end{tikzcd}$$

$$E_K \approx t_T \left(K_M S^2 - \beta \,|\, F_z \,| \right)$$

$$"S" = "B"$$

$$\downarrow$$

$$\mathrm{Ri}_C \approx 0.25$$

$$B \equiv \beta F_z = -\beta \left(2 t_T E_z \right) \frac{\partial \overline{\Theta}}{\partial z}$$

$$\beta = \frac{g}{T_0}$$

$$\mathrm{Ri} = \frac{N^2}{S^2}$$

$$N^2 = \beta \frac{\partial \overline{\Theta}}{\partial z}$$

Budget Equations for Stably Stratified Turbulence

- Turbulent kinetic energy: $E_K = \frac{1}{2}\left\langle \mathbf{u}^2 \right\rangle$
- Potential temperature fluctuations: $E_\theta = \frac{1}{2}\left\langle \theta^2 \right\rangle$
- Flux of potential temperature: $\mathbf{F} = \left\langle \mathbf{u}\,\theta \right\rangle$

$$\frac{DE_K}{Dt} + \operatorname{div}(\boldsymbol{\Phi}_u) - \Pi - \beta F_z = -D_K$$

$$\frac{DE_\theta}{Dt} + \operatorname{div}(\boldsymbol{\Phi}_\theta) + \frac{N^2}{\beta} F_z = -D_\theta$$

$$\frac{DF_i}{Dt} + \operatorname{div}_j(\Phi_{ij}^F) + (\mathbf{F}\cdot\nabla)\overline{U}_i + \frac{N^2}{\beta}\tau_{ij} e_j - 2C_\theta \beta e_i E_\theta = -D_i^F$$

$$\tau_{ij} \equiv \left\langle u_i u_j \right\rangle$$

$$C_\theta \beta_i \left\langle \theta^2 \right\rangle = \beta_i \left\langle \theta^2 \right\rangle + \frac{1}{\rho_0}\left\langle \theta \nabla_i p \right\rangle$$

$$D_K = \frac{E_K}{t_T} \qquad D_\theta = \frac{E_\theta}{C_\theta t_T} \qquad D_i^F = \frac{F_i}{C_F t_T}$$

$$\Pi = -\tau_{ij} \nabla_j \overline{U}_i = K_M S^2$$

Budget Equations for Stably Stratified Turbulence

$$\frac{DE_K}{Dt} + \frac{\partial \Phi_K}{\partial z} = \Pi + \beta F_z - D_K$$

$$\frac{DE_P}{Dt} + \frac{\partial \Phi_P}{\partial z} = -\beta F_z - D_P$$

$$E_\theta = \frac{1}{2}\left\langle \theta^2 \right\rangle$$

$$D_K = \frac{E_K}{t_T}$$

$$D_P = \frac{E_P}{C_P\, t_T}$$

$$E_p \equiv \frac{g}{\rho_0}\left\langle \int \rho\, dz \right\rangle = \left(\frac{\beta}{N}\right)^2 E_\theta = \frac{1}{2}\left(\frac{\beta}{N}\right)^2 \left\langle \theta^2 \right\rangle$$

Total Turbulent Energy

$$\frac{DE}{Dt} + \nabla \cdot \mathbf{\Phi} = \Pi - \frac{E}{C_u\, t_T}$$

$$E = E_K + \left(\frac{\beta}{N}\right)^2 E_\theta$$

The turbulent potential energy:

$$\boxed{E_P = \left(\frac{\beta}{N}\right)^2 E_\theta}$$

Production of Turbulent energy:

$$\Pi = -\tau_{ij} \nabla_j \bar{U}_i = K_M S^2$$

$$K_M = 2 C_\tau A_z\, l \sqrt{E_K}$$

Budget Equations for Stably Stratified Turbulence

$$\frac{DE_K}{Dt} + \frac{\partial \Phi_K}{\partial z} = \Pi + \beta F_z - D_K$$

$$\frac{DE_P}{Dt} + \frac{\partial \Phi_P}{\partial z} = -\beta F_z - D_P$$

$$\frac{DF_z}{Dt} + \frac{\partial \Phi_F}{\partial z} = -D_z^F - \langle u_z u_z \rangle \frac{\partial \overline{\Theta}}{\partial z} + 2C_\theta \beta E_\theta$$

$$E_p \equiv (\beta / N)^2 E_\theta = \tfrac{1}{2} (\beta / N)^2 \overline{\theta'^2}$$

$$C_\theta \beta_i \langle \theta^2 \rangle = \beta_i \langle \theta^2 \rangle + \frac{1}{\rho_0} \langle \theta \nabla_i p \rangle$$

No Critical Richardson Number

$$
\begin{tikzcd}
\boxed{S} \arrow[r] & \boxed{TKE} \arrow[r] \arrow[d] & \boxed{D_K} & \\
& \boxed{B} \arrow[r] & \boxed{\tfrac{1}{2}\left\langle \theta^2 \right\rangle} \arrow[r] \arrow[l, bend left] & \boxed{D_P}
\end{tikzcd}
$$

$$\frac{DE_K}{Dt} + \frac{\partial \Phi_K}{\partial z} = \Pi + \beta\, F_z - D_K$$

$$\frac{DE_P}{Dt} + \frac{\partial \Phi_P}{\partial z} = -\beta F_z - D_P$$

$$C_\theta\, \beta_i \left\langle \theta^2 \right\rangle = \beta_i \left\langle \theta^2 \right\rangle + \frac{1}{\rho_0} \left\langle \theta \nabla_i\, p \right\rangle$$

$$B \equiv \beta\, F_z = -(2E_z\, t_T)\, \frac{\partial \bar{\Theta}}{\partial z} + C_\theta\, \beta^2 \left\langle \theta^2 \right\rangle t_T$$

Comparisons

$$Ri = Pr_{\mathrm{T}} Ri_{\mathrm{f}} = \frac{C_\tau}{C_{\mathrm{F}}} Ri_{\mathrm{f}} \left(1 - \frac{Ri_{\mathrm{f}}(1 - R_\infty) A_z^{(\infty)}}{R_\infty (1 - Ri_{\mathrm{f}}) A_z(Ri_{\mathrm{f}})}\right)^{-1}$$

$$\mathrm{Ri}_f \equiv -\frac{\beta F_z}{\Pi}$$

$$\mathrm{Ri} = \frac{N^2}{S^2}$$

$$\mathrm{Pr}_T \equiv \frac{K_M}{K_H} \equiv \frac{\nu_{\mathrm{T}}}{\kappa_{\mathrm{T}}}$$

$$Pr_{\mathrm{T}} \approx Pr_{\mathrm{T}}^{(0)} + \frac{(1 - R_\infty) A_z^{(\infty)}}{R_\infty A_z^{(0)}} Ri.$$

$$Pr_{\mathrm{T}} \approx 0.8 + 0.45 Ri$$

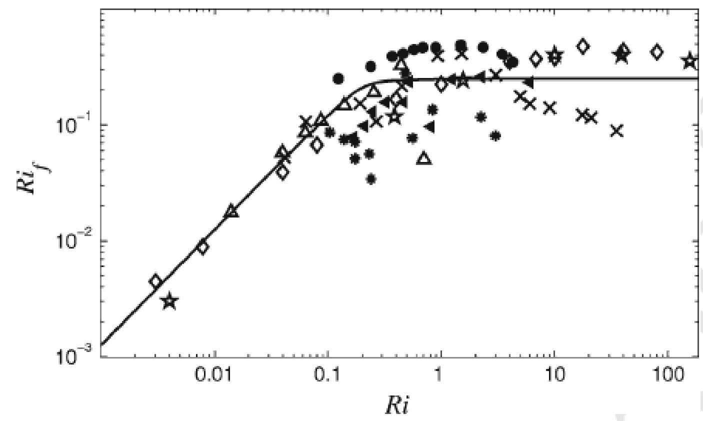

Fig. 4 *Ri*-dependence of the flux Richardson number $Ri_{\mathrm{f}} = -\beta F_z/(\tau S)$ for *meteorological observations*: *slanting black triangles* (Kondo et al. 1978), *snowflakes* (Bertin et al. 1997); *laboratory experiments*: *slanting crosses* (Rehmann and Koseff 2004), *diamonds* (Ohya 2001), *black circles* (Strang and Fernando 2001); *DNS*: *five-pointed stars* (Stretch et al. 2001); *LES*: *triangles* (our DATABASE64). *Solid line* shows the steady-state EFB model, Eq. 56, with $Ri_{\mathrm{f}} \to R_\infty = 0.25$ at $Ri \to \infty$

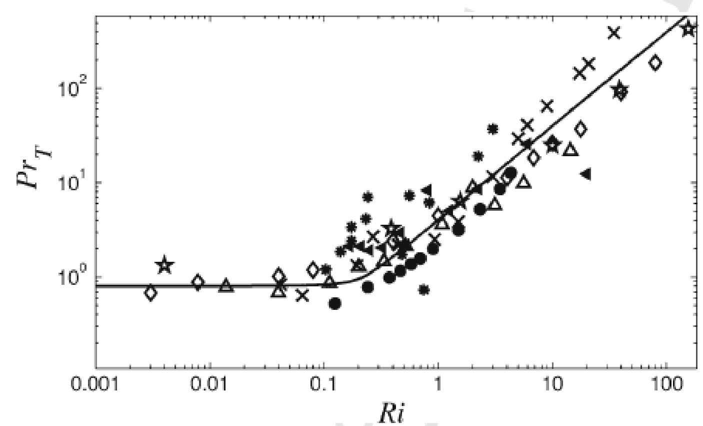

Fig. 5 *Ri*-dependence of the turbulent Prandtl number $Pr_{\mathrm{T}} = K_{\mathrm{M}}/K_{\mathrm{H}}$, after the same data as in Fig. 4 (meteorological observations, laboratory experiments, DNS, and LES). Solid line shows the steady-state EFB model, Eq. 56

Comparisons

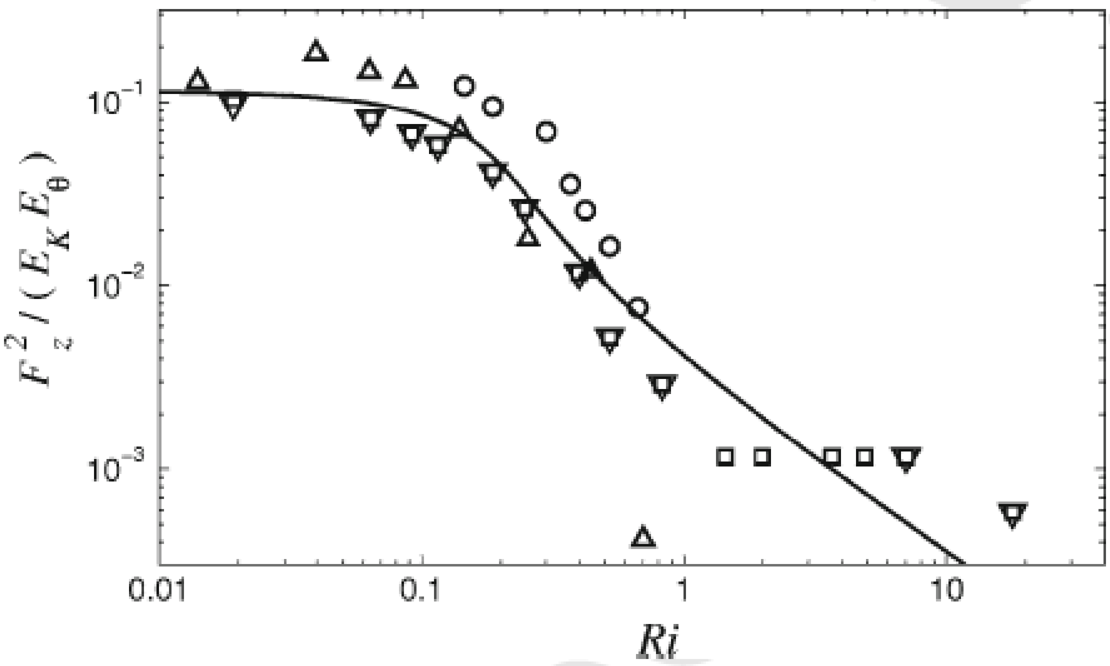

Fig. 9 *Ri*-dependence of the squared dimensionless turbulent flux of potential temperature $F_z^2/(E_K E_\theta)$, for *meteorological observations*: *squares* (CME), *circles* (SHEBA), *overturned triangles* (CASES-99); *laboratory experiments*: *diamonds* (Ohya 2001); LES: *triangles* (our DATABASE64). *Solid line* shows the steady-state EFB model, Eq. 61

$$\mathrm{Ri} = \frac{N^2}{S^2}$$

$$\frac{F_z^2}{E_K E_\theta} = \frac{2C_\tau}{C_P}\frac{A_z(Ri_f)}{Pr_T}.$$

Comparisons

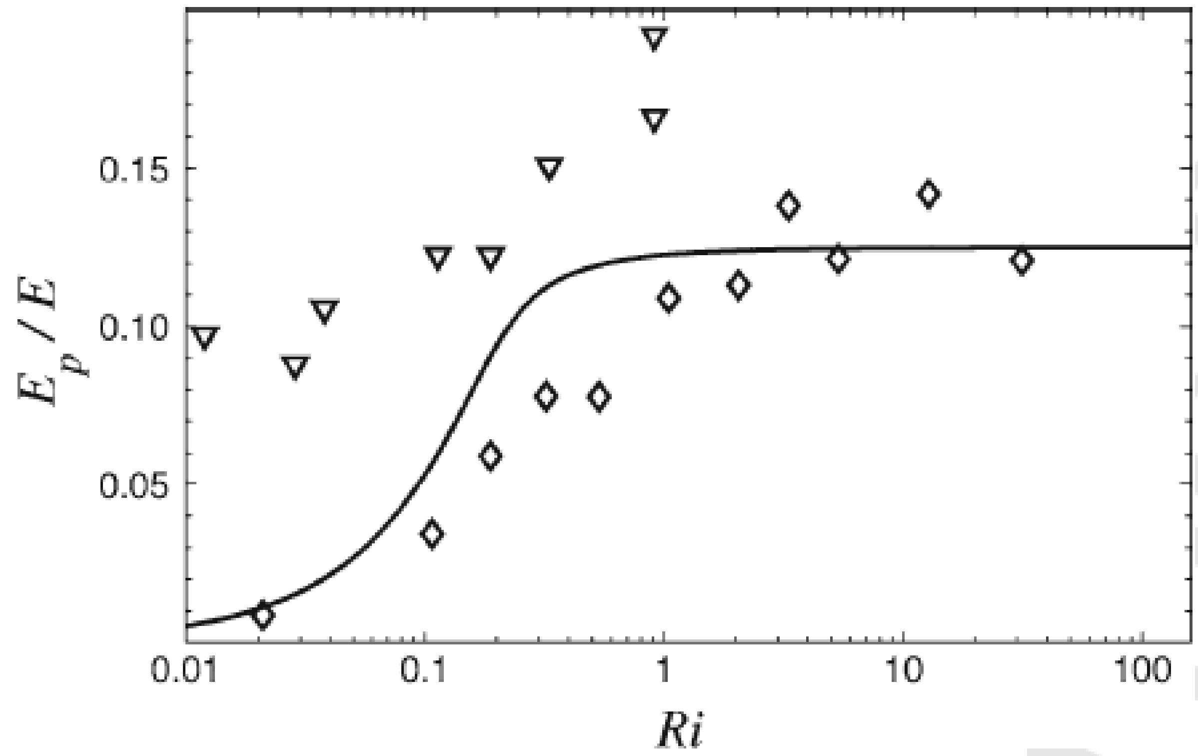

Fig. 7 *Ri*-dependence of the potential-to-total turbulent energy ratio E_P/E, for *meteorological observations*: *overturned triangles* (CASES-99), and *laboratory experiments*: *diamonds* (Ohya 2001). *Solid line* shows the steady-state EFB model, Eqs. 54, 56

$$\frac{E_P}{E} = \frac{C_P Ri_f}{1-(1-C_P)Ri_f}.$$

$$E = E_K + E_p \qquad \mathrm{Ri} = \frac{N^2}{S^2}$$

$$Ri = Pr_T Ri_f = \frac{C_\tau}{C_F} Ri_f \left(1 - \frac{Ri_f(1-R_\infty)A_z^{(\infty)}}{R_\infty(1-Ri_f)A_z(Ri_f)}\right)^{-1}$$

Large-Scale Internal Gravity Waves (IGW)

Basic Equations:

$$\frac{\partial \mathbf{V}^W}{\partial t} = -(\mathbf{U}\cdot\nabla)\mathbf{V}^W - \nabla\left(\frac{P^W}{\rho_0}\right) + \beta\Theta^W\mathbf{e} - \left(\mathbf{V}^W\cdot\nabla\right)\mathbf{V}^W,$$

$$\frac{\partial \Theta^W}{\partial t} = -(\mathbf{U}\cdot\nabla)\Theta^W - \frac{1}{\beta}\left(\mathbf{V}^W\cdot\mathbf{e}\right)N^2 - \left(\mathbf{V}^W\cdot\nabla\right)\Theta^W,$$

Solutions of the Linearized Equations for propagating IGW:

$$V_\alpha^W = -\frac{k_\alpha k_z}{k_h^2}V_0^W(\mathbf{k})\cos(\omega t - \mathbf{k}\cdot\mathbf{r}),$$

$$V_3^W \equiv V_z^W = V_0^W(\mathbf{k})\cos(\omega t - \mathbf{k}\cdot\mathbf{r}),$$

$$\Theta^W = -\frac{Nk}{\beta k_h}V_0^W(\mathbf{k})\sin(\omega t - \mathbf{k}\cdot\mathbf{r})$$

for $\alpha = 1, 2,$

Propagation of IGW in WKB:

$$\frac{\partial \mathbf{r}}{\partial t} = \frac{\partial \omega}{\partial \mathbf{k}},$$

$$\frac{\partial \mathbf{k}}{\partial t} = -\frac{\partial \omega}{\partial \mathbf{r}},$$

Frequency of IGW:

$$\omega = \frac{k_h}{k}N + \mathbf{k}\cdot\mathbf{U},$$

$$N^2 = \beta\frac{\partial\overline{\Theta}}{\partial z}$$

$\mathbf{k}_h$ =constant

$$\frac{k_h}{k(z)}N(z) + \mathbf{k}\cdot(\mathbf{U}(z) - \mathbf{U}(Z_0)) = \frac{k_h}{k_0}N(Z_0),$$

Sources for Internal Gravity Waves

- Random convective motions underlying the stably stratified turbulence.
- Strong large-scale shear.
- Large-scale flows over complex terrain.
- Wave-wave interactions.

Large-Scale Internal Gravity Waves (IGW)

- We consider the large-scale IGW with random phases whose periods and wave lengths are much larger than the turbulent time and length scales.
- We represent the total velocity as the sum of the mean-flow velocity, the turbulent velocity, and the wave-field velocity:

$$\mathbf{v} = \mathbf{U} + \mathbf{u} + \mathbf{V}^W,$$

- We neglect the wave-wave interactions at large scales, but take into account the turbulence-wave interactions.
- We assume that the energy spectrum of the ensemble of IGW is isotropic and has the power-law form: $e_W(k_0) = (\mu - 1) E_W H^{-(\mu+1)} k_0^{-\mu},$

where $E_W = \int [e_W(\mathbf{k}_0)/2\pi k_0^2] d\mathbf{k}_0 = \int e_W(k_0) dk_0$

Large-Scale Internal Gravity Waves with Random phases

$$\frac{DE_K}{Dt} + \frac{\partial \Phi_K}{\partial z} = -\tau_{i3}\frac{\partial U_i}{\partial z} + \beta F_z - \varepsilon_K - \left\langle \tau_{ij}^W \frac{\partial V_i^W}{\partial x_j} \right\rangle_W + \beta \left\langle V_z^W \, \Theta^W \right\rangle_W ,$$

$$\frac{DE_\theta}{Dt} + \frac{\partial \Phi_\theta}{\partial z} = -F_z \frac{\partial \Theta}{\partial z} - \varepsilon_\theta - \left\langle F_j^W \frac{\partial \Theta^W}{\partial x_j} \right\rangle_W ,$$

$$\frac{DF_i}{Dt} + \frac{\partial}{\partial x_j}\Phi_{ij}^{(F)} = \beta_i \left\langle \theta^2 \right\rangle + \frac{1}{\rho_0}\left\langle \theta \nabla_i p \right\rangle - \tau_{i3}\frac{\partial \Theta}{\partial z} - F_j \frac{\partial U_i}{\partial x_j} - \varepsilon_i^{(F)} - \left\langle \tau_{ij}^W \frac{\partial \Theta^W}{\partial x_j} \right\rangle_W$$
$$- \left\langle F_j^W \frac{\partial V_i^W}{\partial x_j} \right\rangle_W .$$

where

$$F_i^W \approx -C_F t_T \left(\tau_{ij} \frac{\partial \Theta^W}{\partial x_j} + \tau_{i3}^W \frac{\partial \Theta}{\partial z} + F_j \frac{\partial V_i^W}{\partial x_j} \right).$$

$$\tau_{ij}^W \approx -C_\tau t_T \left(\tau_{ik} \frac{\partial V_j^W}{\partial x_k} + \tau_{jk} \frac{\partial V_i^W}{\partial x_k} \right).$$

Budget Equations for SST with Large-Scale Internal Gravity Waves

$$\omega = \frac{k_h}{k} N$$

$$\frac{DE_K}{Dt} + \frac{\partial \Phi_K}{\partial z} = \Pi + \beta F_z - \frac{E_K}{t_T} + \prod^{W}$$

$$\frac{DE_P}{Dt} + \frac{\partial \Phi_P}{\partial z} = -\beta F_z - \frac{E_P}{C_P t_T} + \prod_{P}^{W}$$

$$\frac{DF_z}{Dt} + \frac{\partial \Phi_F}{\partial z} = -\left\langle u_z^2 \right\rangle \frac{\partial \bar{\Theta}}{\partial z} + 2C_\theta \beta E_\theta - \frac{F_z}{C_F t_T} + \sqcap_F^W$$

$$\sqcap^W = \sqcap^W \left(\frac{E_W}{S^2 H^2}, \frac{N(z)}{N(z_0)} \right)$$

Turbulent Prandtl Number vs. Ri (IG-Waves)

$$\Pr_T \equiv \frac{K_M}{K_H}$$

$$G \propto \frac{E^W}{S^2 H^2}$$

$$Q = \frac{N^2(z)}{N^2(z_0)}$$

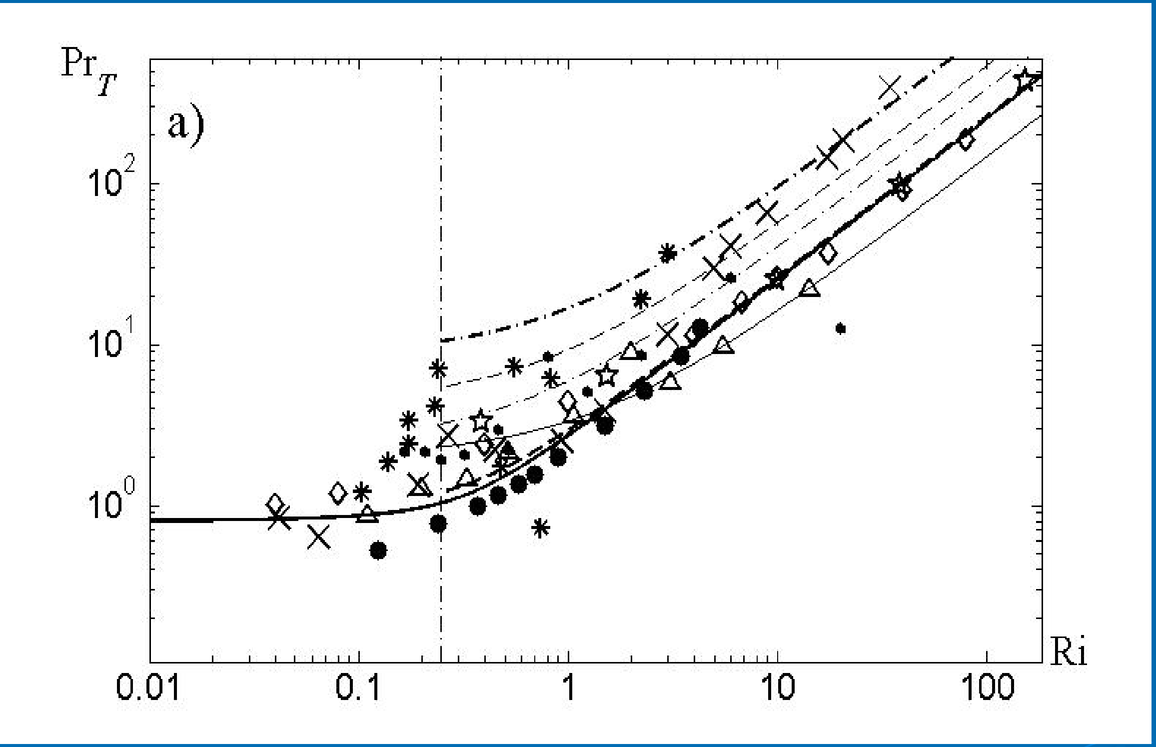

Meteorological observations: slanting black triangles (Kondo et al., 1978), snowflakes (Bertin et al., 1997); laboratory experiments: black circles (Strang and Fernando, 2001), slanting crosses (Rehmann and Koseff, 2004), diamonds (Ohya, 2001); LES: triangles (Zilitinkevich et al., 2008); DNS: five-pointed stars (Stretch et al., 2001). Our model with IG-waves at Q=10 and different values of parameter G: G=0.01 (thick dashed), G= 0.1 (thin dashed-dotted), G=0.15 (thin dashed), G=0.2 (thick dashed-dotted), at Q=1 for G=1 (thin solid) and without IG-waves at G=0 (thick solid).

Ri_f vs. Ri (IG-Waves)

$$\boxed{\mathrm{Ri}_f \equiv -\frac{\beta F_z}{\Pi}}$$

$$G \propto \frac{E^W}{S^2 H^2}$$

$$Q = \frac{N^2(z)}{N^2(z_0)}$$

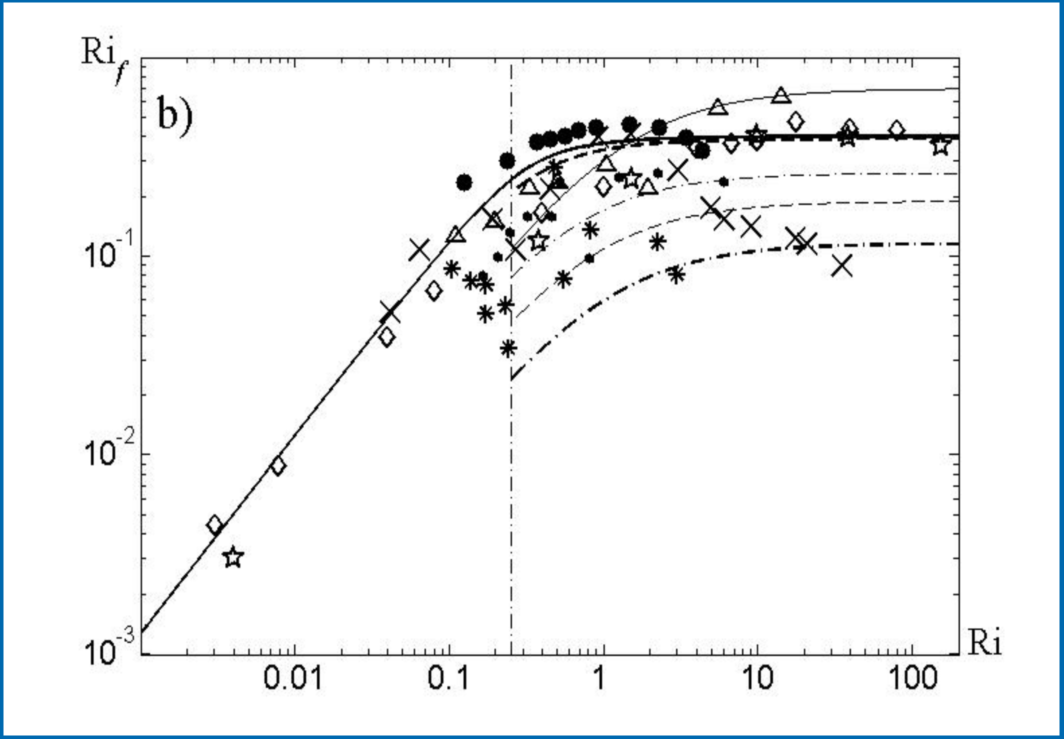

Meteorological observations: slanting black triangles (Kondo et al., 1978), snowflakes (Bertin et al., 1997); laboratory experiments: black circles (Strang and Fernando, 2001), slanting crosses (Rehmann and Koseff, 2004), diamonds (Ohya, 2001); LES: triangles (Zilitinkevich et al., 2008); DNS: five-pointed stars (Stretch et al., 2001). Our model with IG-waves at Q=10 and different values of parameter G: G=0.01 (thick dashed), G= 0.1 (thin dashed-dotted), G=0.15 (thin dashed), G=0.2 (thick dashed-dotted), at Q=1 for G=1 (thin solid); and without IG-waves at G=0 (thick solid).

F_z vs. Ri (IG-Waves)

$$F_z = -K_H \frac{\partial \bar{\Theta}}{\partial z} + 2C_\theta \beta E_\theta t_T$$

$$G \propto \frac{E^W}{S^2 H^2}$$

$$Q = \frac{N^2(z)}{N^2(z_0)}$$

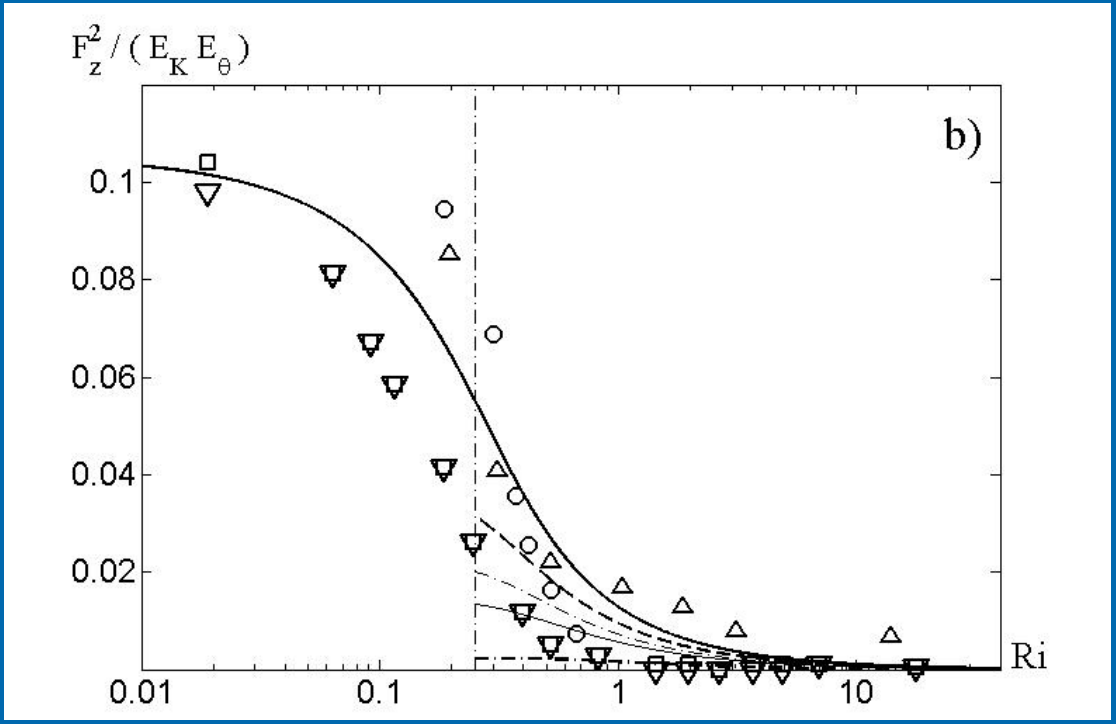

Meteorological observations: squares [CME, Mahrt and Vickers (2005)], circles [SHEBA, Uttal et al. (2002)], overturned triangles [CASES-99, Poulos et al. (2002), Banta et al. (2002)], slanting black triangles (Kondo et al., 1978), snowflakes (Bertin et al., 1997); laboratory experiments: black circles (Strang and Fernando, 2001), slanting crosses (Rehmann and Koseff, 2004), diamonds (Ohya, 2001); LES: triangles (Zilitinkevich et al., 2008); DNS: five-pointed stars (Stretch et al., 2001). Our model with IG-waves at Q=10 and different values of parameter G: G=0.001 (thin dashed), G=0.005 (thick dashed), G= 0.01 (thin dashed-dotted), G=0.05 (thick dashed-dotted), at Q=1 for G=0.1 (thin solid); and without IG-waves at G=0 (thick solid).

$\frac{E_p}{E}$ vs. Ri (IG-Waves)

$$\boxed{E = E_K + E_p}$$

$$G \propto \frac{E^W}{S^2 H^2}$$

$$Q = \frac{N^2(z)}{N^2(z_0)}$$

$$\frac{E^W}{E} = \frac{2E_p}{E} = 0.2 - 0.8$$

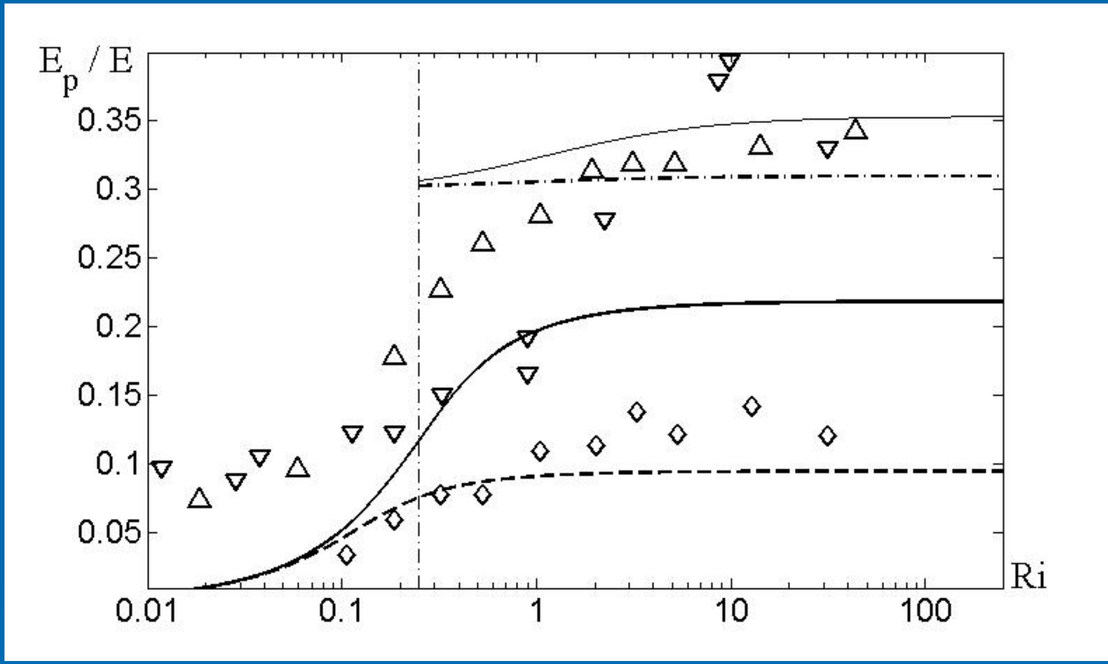

Meteorological observations: overturned triangles [CASES-99, Poulos et al. (2002), Banta et al. (2002)]; laboratory experiments: diamonds (Ohya, 2001); LES: triangles (Zilitinkevich et al., 2008). Our model with IG-waves at Q=10 and different values of parameter G: G=0.2 (thick dashed-dotted), at Q=1 for G=1 (thin solid); and without IG-waves at G=0 (thick solid for $\mathrm{Ri}_f^{\infty} = 0.4$) and (thick dashed for $\mathrm{Ri}_f^{\infty} = 0.2$).

Large-Scale Internal Gravity Waves (Two-way Coupling)

$$\frac{DE_K}{Dt} + \frac{\partial \Phi_K}{\partial z} = -\tau_{i3}\frac{\partial U_i}{\partial z} + \beta F_z - \varepsilon_K - \left\langle \tau_{ij}^W \frac{\partial V_i^W}{\partial x_j} \right\rangle_W + \beta \left\langle V_z^W \Theta^W \right\rangle_W ,$$

$$\frac{DE_\theta}{Dt} + \frac{\partial \Phi_\theta}{\partial z} = -F_z \frac{\partial \Theta}{\partial z} - \varepsilon_\theta - \left\langle F_j^W \frac{\partial \Theta^W}{\partial x_j} \right\rangle_W ,$$

$$\frac{DF_i}{Dt} + \frac{\partial}{\partial x_j}\Phi_{ij}^{(F)} = \beta_i \left\langle \theta^2 \right\rangle + \frac{1}{\rho_0}\left\langle \theta \nabla_i p \right\rangle - \tau_{i3}\frac{\partial \Theta}{\partial z} - F_j \frac{\partial U_i}{\partial x_j} - \varepsilon_i^{(F)} - \left\langle \tau_{ij}^W \frac{\partial \Theta^W}{\partial x_j} \right\rangle_W$$

$$- \left\langle F_j^W \frac{\partial V_i^W}{\partial x_j} \right\rangle_W .$$

where

$$F_i^W \approx -C_F t_T \left(\tau_{ij} \frac{\partial \Theta^W}{\partial x_j} + \tau_{i3}^W \frac{\partial \Theta}{\partial z} + F_j \frac{\partial V_i^W}{\partial x_j} \right).$$

$$\tau_{ij}^W \approx -C_\tau t_T \left(\tau_{ik} \frac{\partial V_j^W}{\partial x_k} + \tau_{jk} \frac{\partial V_i^W}{\partial x_k} \right).$$

Budget Equations for IGW: S=0

$$\frac{DE_K^W}{Dt} + \operatorname{div}\mathbf{\Phi}^W = \left\langle \tau_{ij}^W \frac{\partial V_i^W}{\partial x_j} \right\rangle_W ,$$

$$\frac{DE_P^W}{Dt} = \frac{\beta^2}{N^2} \left\langle F_j^W \frac{\partial \Theta^W}{\partial x_j} \right\rangle_W ,$$

where

$$\tau_{ij}^W \approx -C_\tau t_T \left(\tau_{ik} \frac{\partial V_j^W}{\partial x_k} + \tau_{jk} \frac{\partial V_i^W}{\partial x_k} \right).$$

$$F_i^W \approx -C_F t_T \left(\tau_{ij} \frac{\partial \Theta^W}{\partial x_j} + \tau_{i3}^W \frac{\partial \Theta}{\partial z} + F_j \frac{\partial V_i^W}{\partial x_j} \right).$$

$$\mathbf{\Phi}^W = \frac{1}{\rho_0} \left\langle p^W \mathbf{V}^W \right\rangle_W = \int \mathbf{C_g}(\mathbf{k}) \widetilde{E}^W(\mathbf{k})\, d\mathbf{k} ,$$

Total wave energy:

$$E^W = E_K^W + E_p^W ,$$

$$\frac{DE^W}{Dt} + \frac{\partial}{\partial z}\left[V_g(Q) E^W \right] = -\,\gamma_d(E^W)\, E^W$$

where

$$\gamma_d(E^W) = C_F\,(1 + \mathrm{Pr}_0)\, \pi^W \frac{\ell_T}{H^2} \sqrt{E_K(E^W)}$$

$$V_g(Q) = \frac{\mu - 1}{\mu} N_0 H f(Q)$$

Wave Richardson Number

$$\mathrm{Ri}_W = \frac{N_0^2 H^2}{E_W \, \mathrm{Pr}_T^{(0)} \, \Gamma}$$

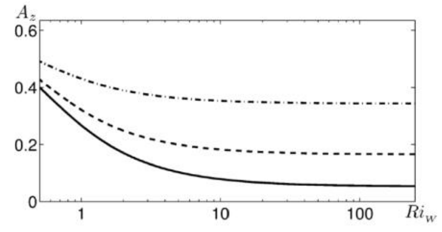

Figure 1. The anisotropy parameter A_z versus the parameter for different values of the parameter C_0: $C_0 = 1/15$ (solid), $C_0 = 0.1$ (dashed), $C_0 = 0.217$ (dashed-doted).

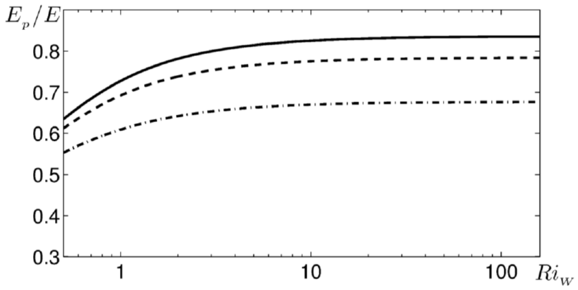

Figure 2. The ratio of potential to the total energy versus the parameter Ri_W.

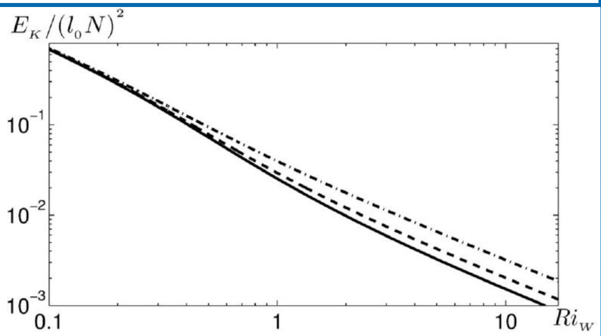

Figure 3. Kinetic energy (in Ozmidov units) versus the parameter Ri_W.

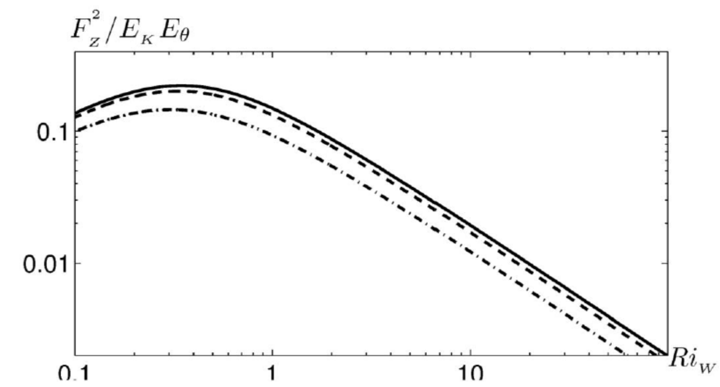

Figure 4. The non-dimensional squared potential temperature flux versus the parameter Ri_W.

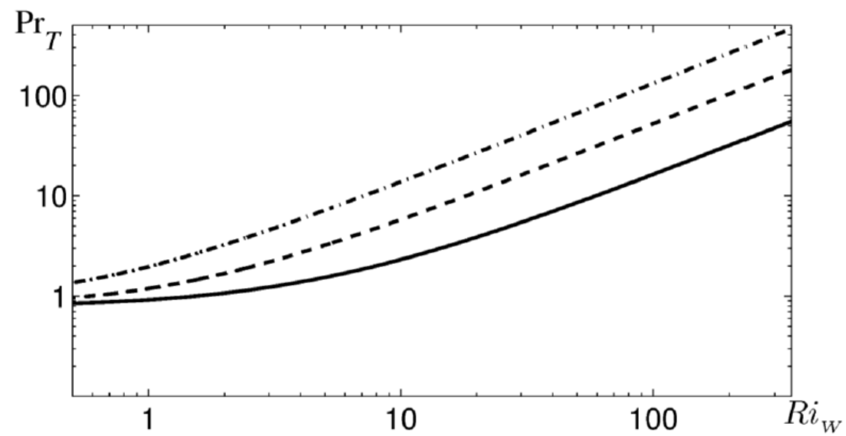

Figure 5. The turbulent Prandtl number Pr_T versus the parameter Ri_W.

Spatial Profiles

$$\mathrm{H}_{eff} = H\frac{\mu - 1}{2\mu\Gamma\sqrt{2C_F^3/3}\left(1+\mathrm{Pr}_0\right)}\left(\frac{H}{\ell_T}\right)^2$$

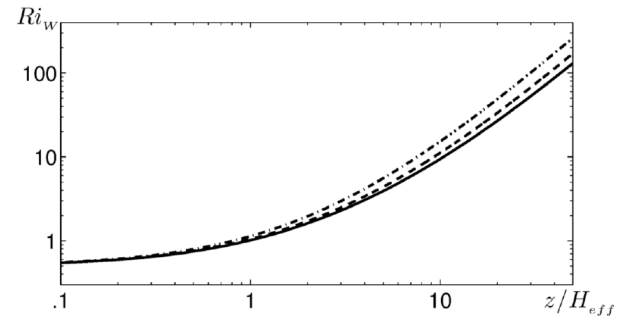

Figure 7. The vertical profile of the parameter $\mathrm{Ri}_W(z)$.

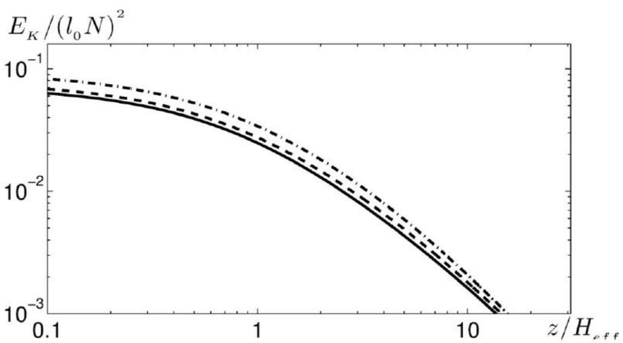

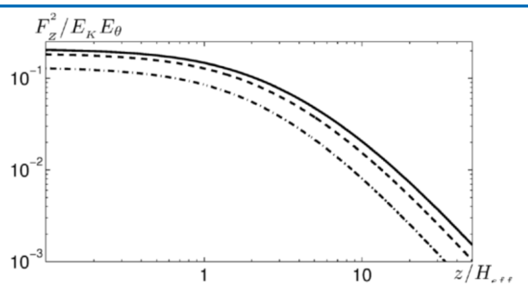

Figure 9. The vertical profile of the non-dimensional squared flux of the potential temperature.

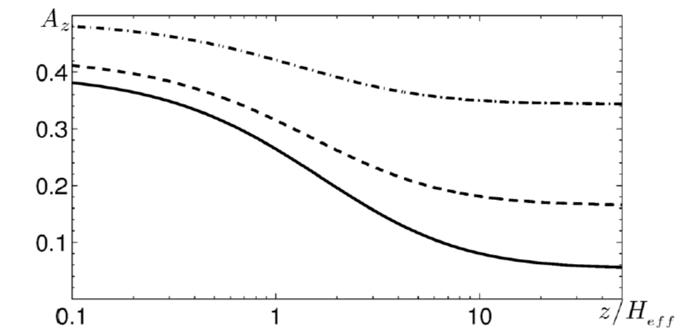

Figure 10. The vertical profile of the anisotropy parameter A_z.

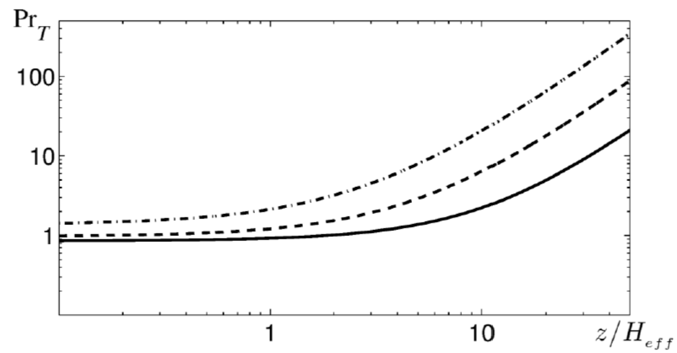

Figure 11. The vertical profile of the turbulent Prandtl number, Pr_T.

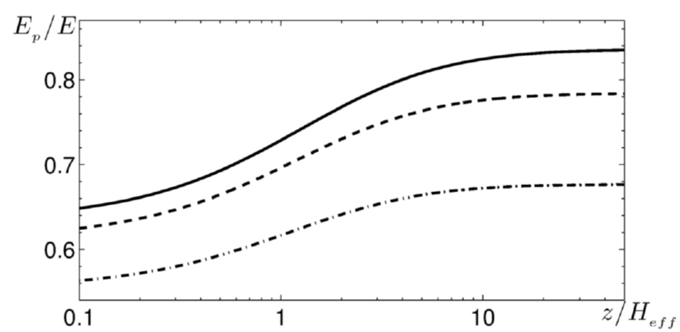

Figure 12. The vertical profile of the ratio of the potential to the total energy.

Laboratory Experiments in Convective turbulence

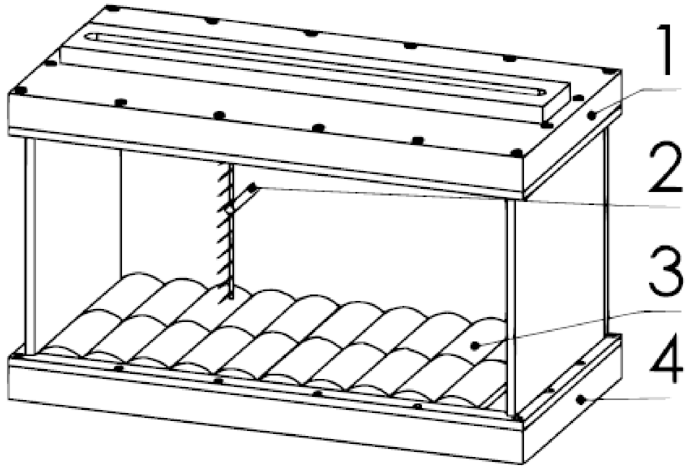

FIG. 2. A sketch of the chamber: heat exchangers at the bottom (4) and top (1) surfaces; temperature probe (2) equipped with 12 E-thermocouples; a wavy bottom surface (3) with a sinusoidal modulation.

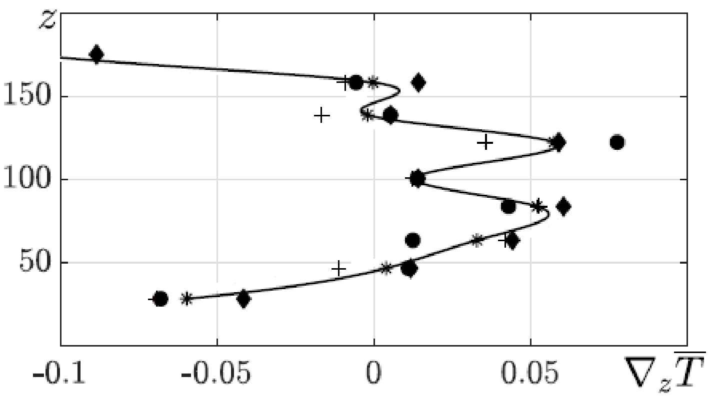

FIG. 5. Profiles of the vertical mean temperature gradient $\nabla_z \overline{T}$ in the experiments with the wavy bottom surface for $\Delta T = 50$ K for different cross-sections on the left at $y = 193.6$

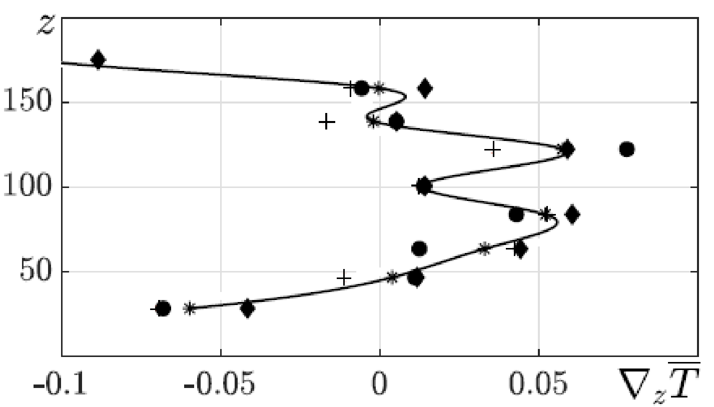

FIG. 6. Profiles of the vertical mean temperature gradient $\nabla_z \overline{T}$ in the experiments with the wavy bottom surface for $\Delta T = 50$ K for different cross-sections on the right at

Standing Internal Gravity Waves (IGW)

$$\frac{\partial \boldsymbol{V}^{\mathrm{W}}}{\partial t} = -\frac{\boldsymbol{\nabla} P^{\mathrm{W}}}{\rho_{\mathrm{eq}}} + g\, S^{\mathrm{W}} \boldsymbol{e},$$
$$\frac{\partial S^{\mathrm{W}}}{\partial t} = -g^{-1} N^2\, \boldsymbol{V}^{\mathrm{W}} \cdot \boldsymbol{e},$$

$$\frac{\partial^2}{\partial t^2} \Delta V_z^{\mathrm{W}} = -N^2(z) \Delta_\perp V_z^{\mathrm{W}},$$
$$\frac{\partial^2}{\partial t^2} \Delta \boldsymbol{V}_\perp^{\mathrm{W}} = \boldsymbol{\nabla}_\perp \nabla_z^2 \left[V_z^{\mathrm{W}} N^2(z) \right].$$

$$\omega = N(z) \frac{k_h}{k}$$

$$\frac{\partial \boldsymbol{r}}{\partial t} = \frac{\partial \omega}{\partial \boldsymbol{k}}, \quad \frac{\partial \boldsymbol{k}}{\partial t} = -\frac{\partial \omega}{\partial \boldsymbol{r}}$$

Solution for standing internal gravity waves in WKB approximation:

$$\boldsymbol{k}_h = \mathrm{const}$$

$$V_z^{\mathrm{W}}(t, \boldsymbol{r}) = V_* \cos(\omega t) \cos(\boldsymbol{k}_h \cdot \boldsymbol{r}) \sin \left(\int_{z_{\min}}^{z} k_z(z')\, dz' + \varphi \right),$$

$$k_z(z) = k_h \left(\frac{N^2(z)}{\omega^2} - 1 \right)^{1/2}$$

$$\boldsymbol{V}_\perp^{\mathrm{W}}(t, \boldsymbol{r}) = -\boldsymbol{k}_h \frac{k_z(z)}{k_h^2} V_* \cos(\omega t) \sin(\boldsymbol{k}_h \cdot \boldsymbol{r}) \cos \left(\int_{z_{\min}}^{z} k_z(z')\, dz' + \varphi \right)$$

$$S^{\mathrm{W}}(t, \boldsymbol{r}) = \frac{N^2(z)}{g\, \omega} V_* \sin(\omega t) \cos(\boldsymbol{k}_h \cdot \boldsymbol{r}) \sin \left(\int_{z_{\min}}^{z} k_z(z')\, dz' + \varphi \right)$$

Boundary conditions:

$$V_z^{\mathrm{W}}(z = z_{\min}) = 0$$
$$V_z^{\mathrm{W}}(z \approx z_{\max}) = 0$$

$$N^2(z) = N_0^2 (1 - z^2/L_N^2)$$

Analogy with quantum mechanics:
the behavior of the wave function $\propto \sin(\int_{z_{\min}}^{z} k_z(z')\, dz' + \pi/4)$
near the turning points: $k_z(z = z_{\max}) = 0$

The Bohr-Sommerfeld quantization condition:

$$\int_{z_{\min}}^{z_{\max}} k_z(z')\, dz' = \pi \left(m + \frac{1}{4} \right)$$

$z_{\max}$ is the reflection (or "turning") point.

The frequencies of the standing IGW:

$$\omega_m = \frac{N_0}{k_h L_N} \left\{ \left[\left(m + \frac{1}{4} \right)^2 + (k_h L_N)^2 \right]^{1/2} - \left(m + \frac{1}{4} \right) \right\},$$

Laboratory Experiments in Convective turbulence

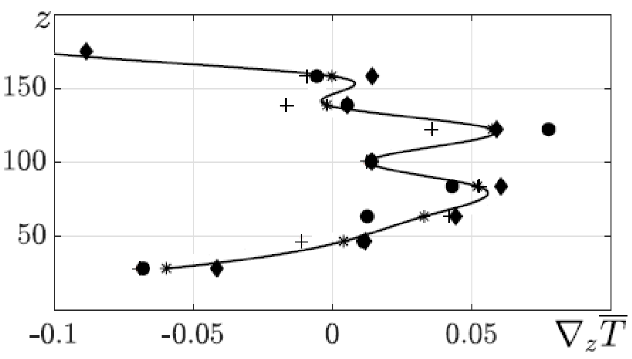

FIG. 5. Profiles of the vertical mean temperature gradient $\nabla_z \overline{T}$ in the experiments with the wavy bottom surface for $\Delta T = 50$ K for different cross-sections on the left at $y = 193.6$

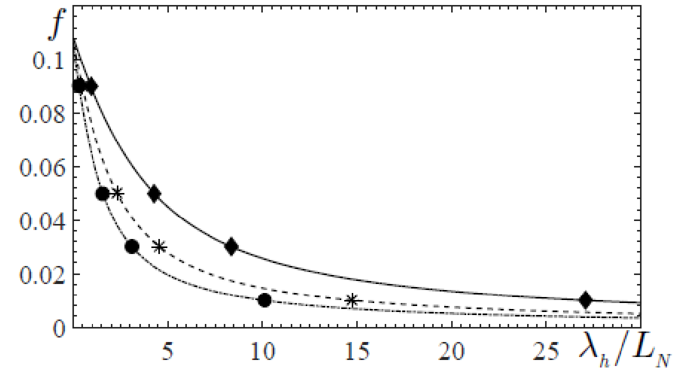

FIG. 6. The frequencies of the internal gravity waves (measured in Hz) versus the normalized horizontal wavelength λ_h / L_N: theoretical curves for different modes $m = 1$ (solid), $m = 2$ (dashed) and $m = 3$ (dashed-dotted) and measured frequencies associated with different modes: $m = 1$ (diamonds), $m = 2$ (snowflakes) and $m = 3$ (circles) in the experiments for the temperature differences $\Delta T = 50$ K between the bottom and top walls.

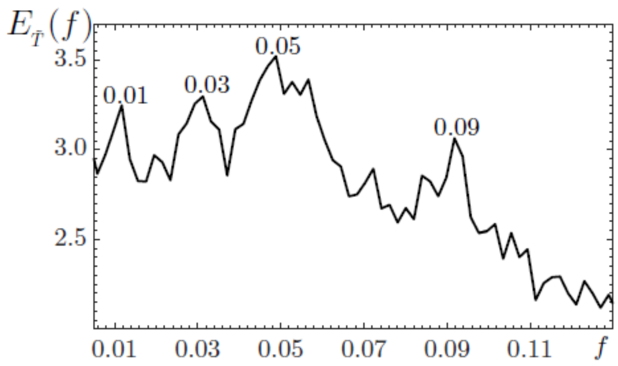

FIG. 9. The averaged spectrum function $E_{\tilde{T}}(f)$ of the temperature field obtained in the experiments for the temperature differences $\Delta T = 50$ K between the bottom and top surfaces.

$$\omega_m = \frac{N_0}{k_h L_N} \left\{ \left[\left(m + \frac{1}{4} \right)^2 + (k_h L_N)^2 \right]^{1/2} - \left(m + \frac{1}{4} \right) \right\},$$

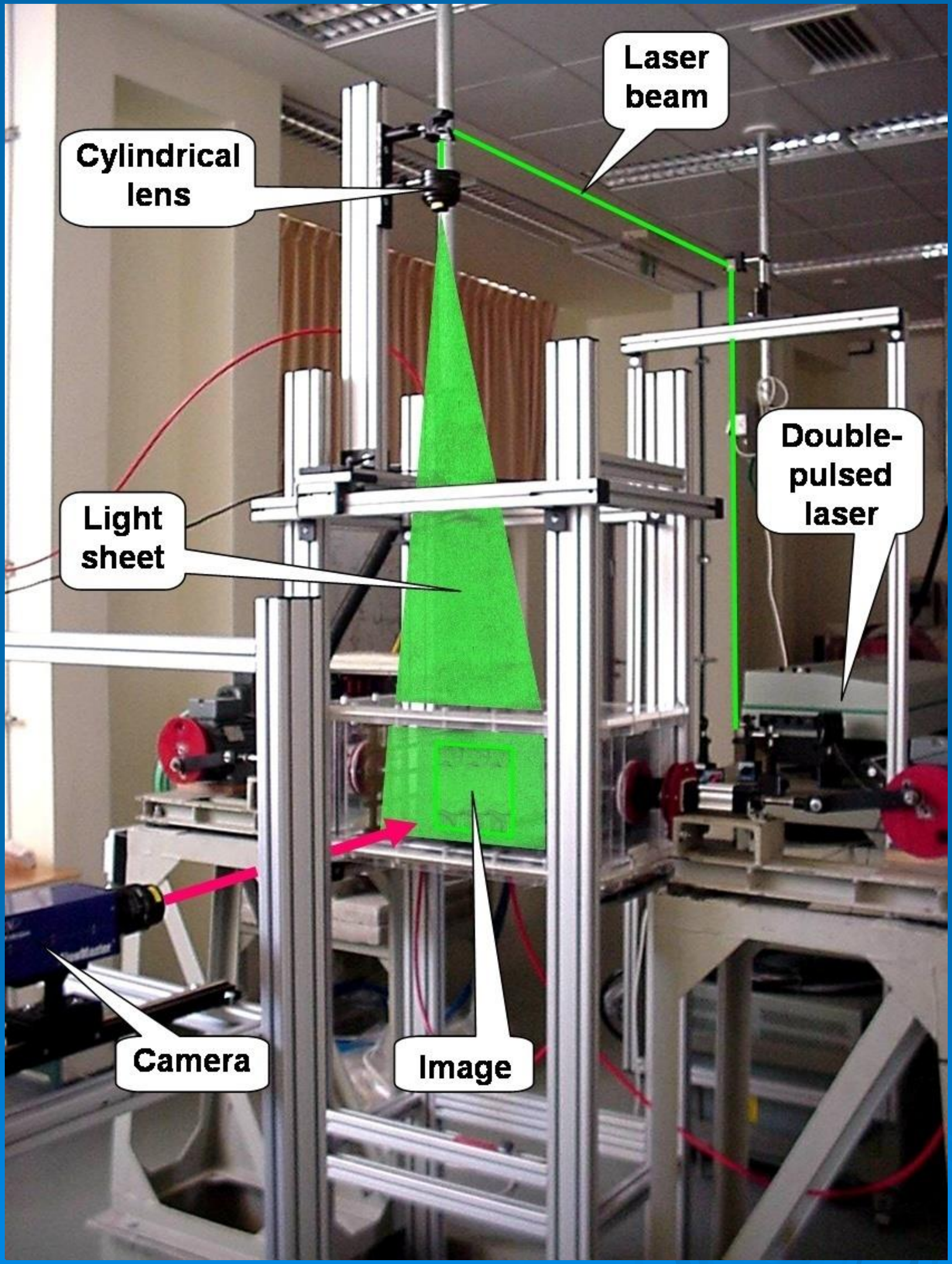

Experimental set - up: oscillating grids turbulence generator and particle image velocimetry system

Particle Image Velocimetry System

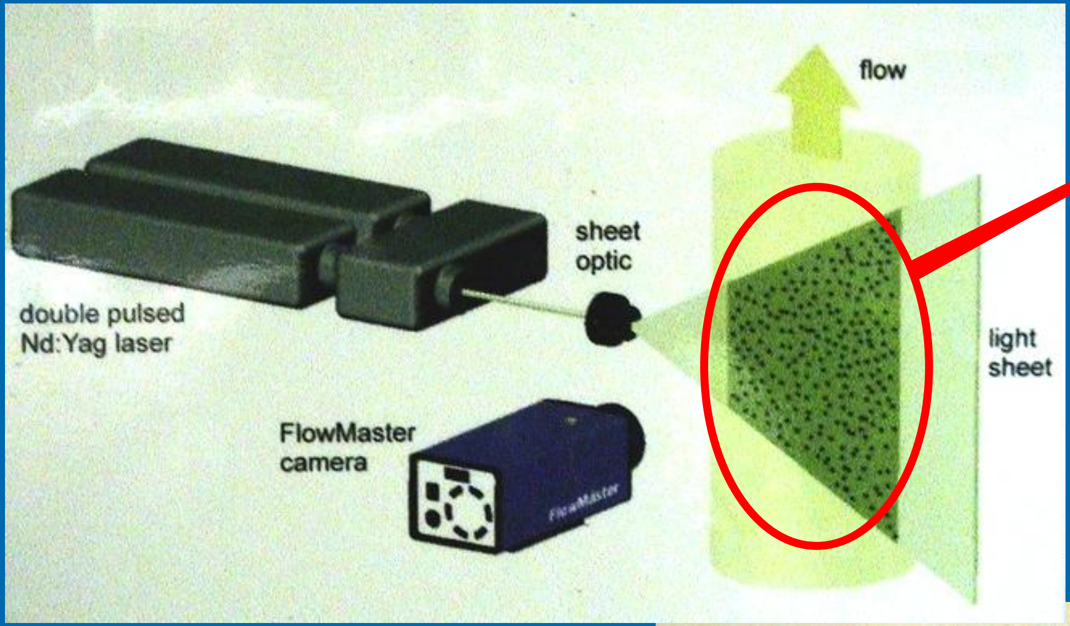

Raw image of the incense smoke tracer particles in oscillating grids turbulence

Particle Image Velocimetry Data Processing

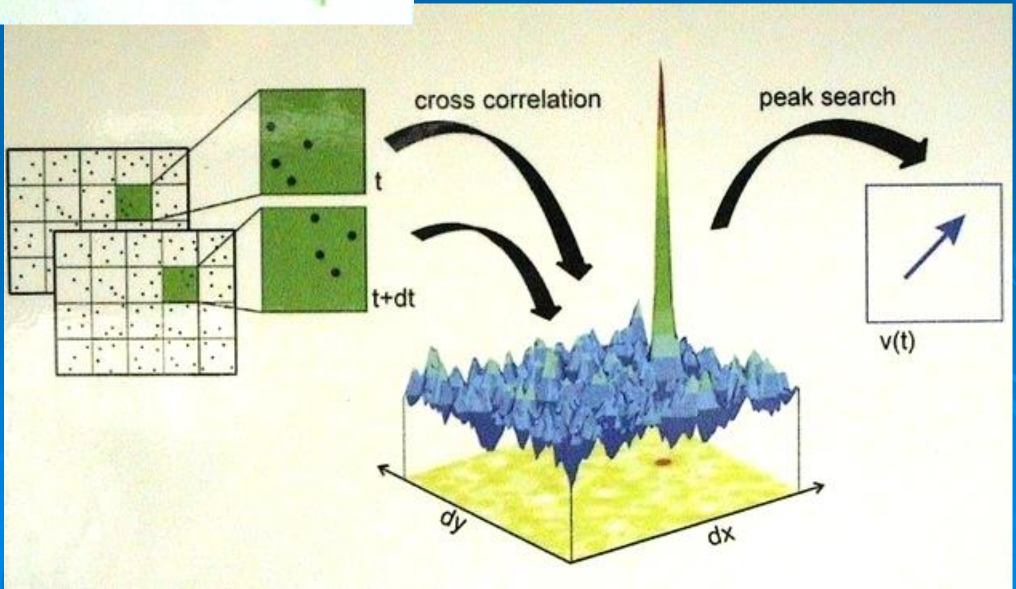

Unforced Convection: A = 1

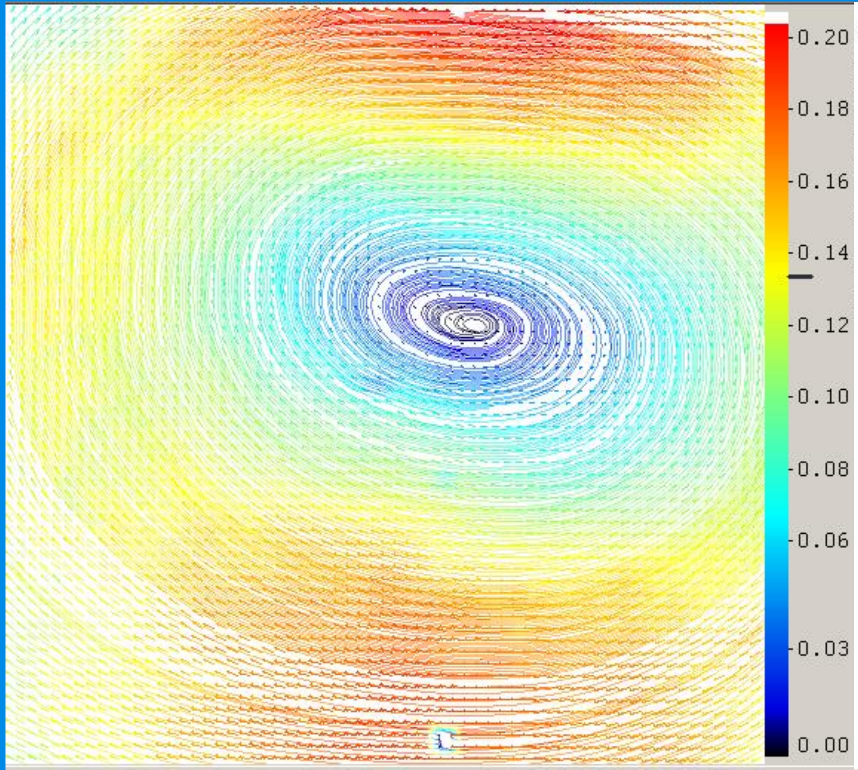

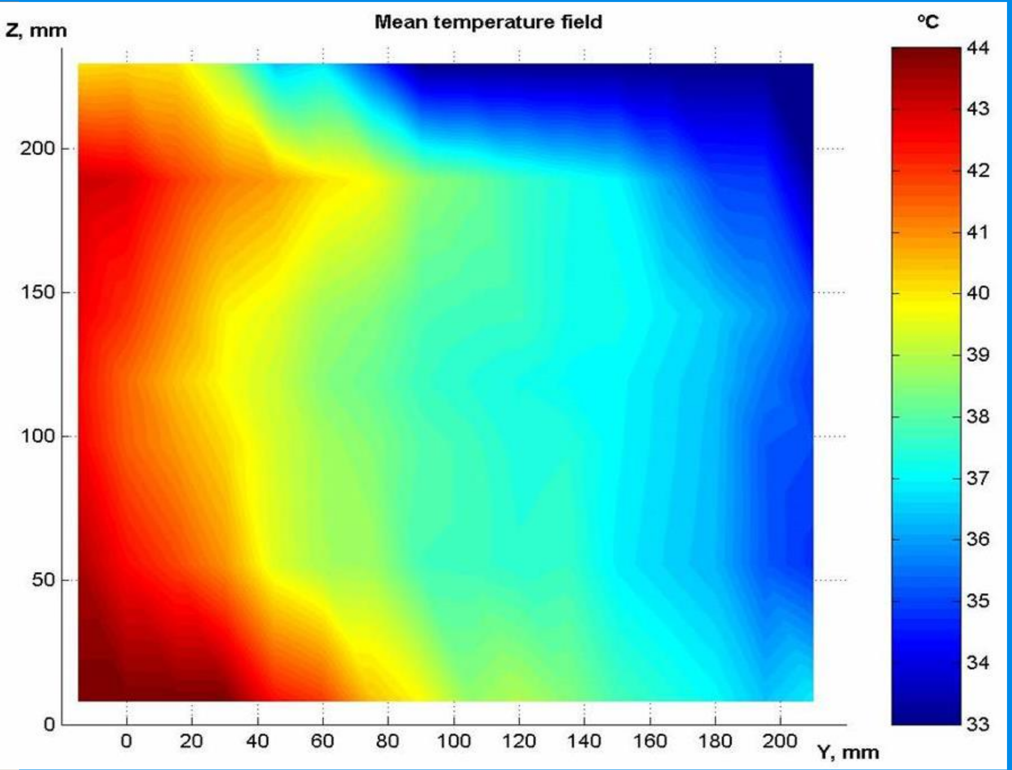

$\overline{U}(y, z)$

$\overline{T}(y, z)$

Temperature Field in Forced and Unforced Turbulent Convection

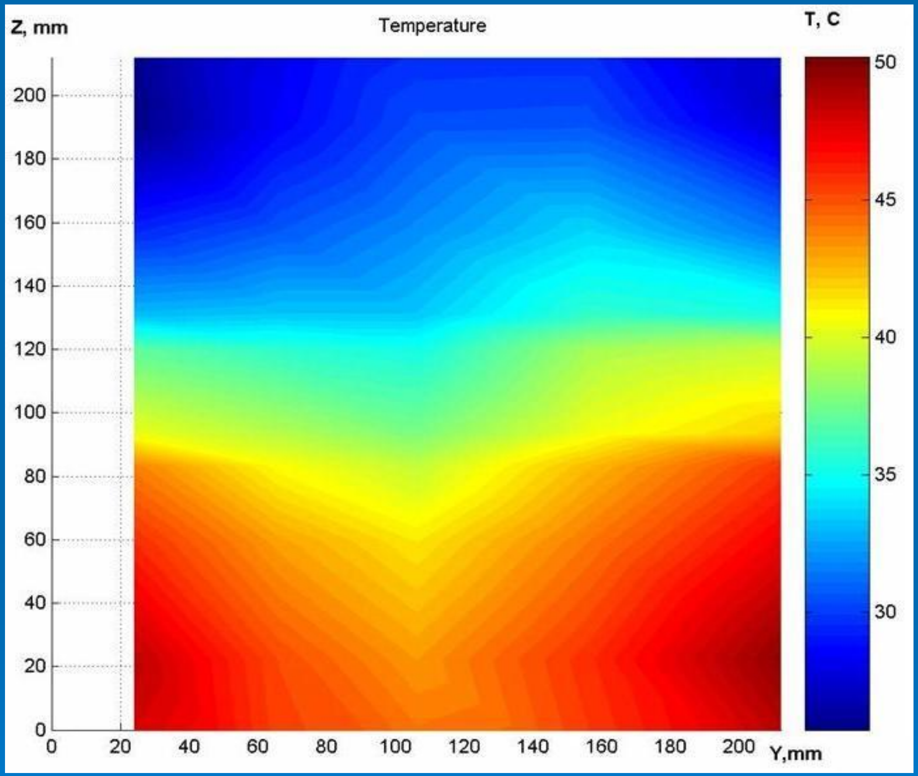

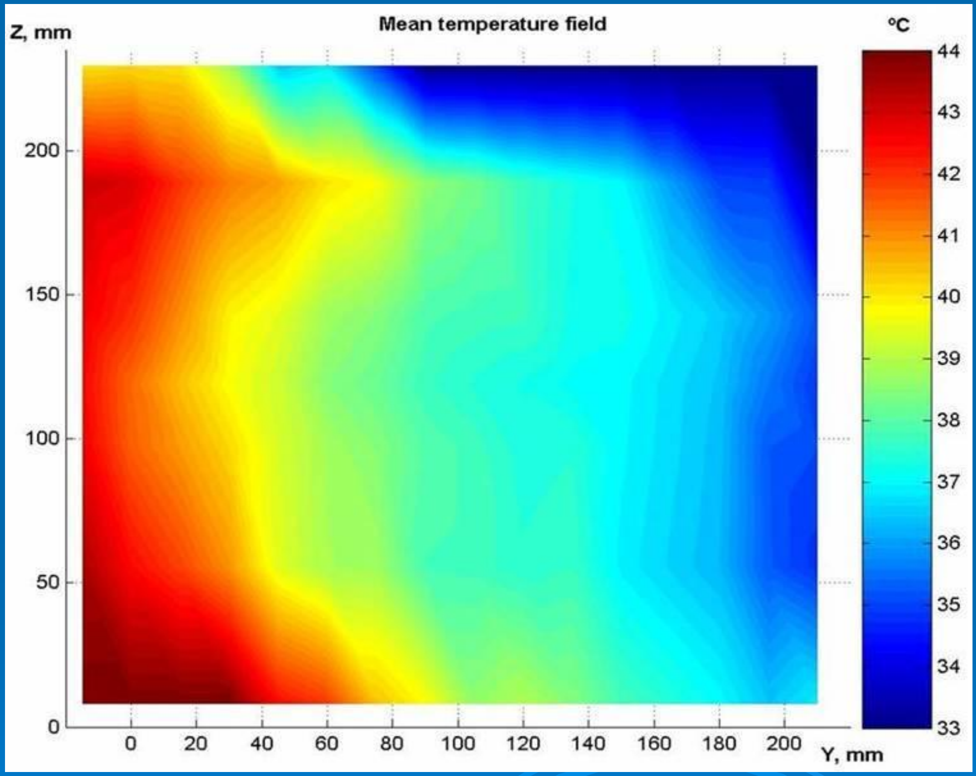

Forced turbulent convection
(two oscillating grids)

Unforced convection

The atmospheric convective boundary layer (CBL) consists in three basic parts:

- ***Surface layer*** strongly unstably stratified and dominated by small-scale turbulence of very complex nature including usual 3-D turbulence, generated by mean-flow surface shear and structural shears ***(the lower part of the surface layer)***, and unusual strongly anisotropic buoyancy-driven turbulence ***(the upper part of the surface layer)***;

- ***CBL core*** dominated by the structural energy-, momentum- and mass-transport, with only minor contribution from usual 3-D turbulence generated by local structural shears on the background of almost zero vertical gradient of potential temperature (or buoyancy);

- ***Turbulent entrainment layer* at the CBL upper boundary**, characterised by essentially stable stratification with negative (downward) turbulent flux of potential temperature (or buoyancy).

Budget Equations for Shear-Free Convection

$$\frac{DE_K}{Dt} + \nabla \cdot \mathbf{\Phi}_K = -\tau_{ij} \frac{\partial U_i}{\partial x_j} + \beta F_z - \varepsilon_K ,$$

$$\frac{DE_\theta}{Dt} + \nabla \cdot \mathbf{\Phi}_\theta = -\left(\mathbf{F} \cdot \nabla\right)\Theta - F_z \frac{\partial \overline{\Theta}}{\partial z} - \varepsilon_\theta ,$$

$$\frac{DF_i}{Dt} + \frac{\partial}{\partial x_j} \Phi_{ij}^{(F)} = \beta \delta_{i3} \left\langle \theta^2 \right\rangle - \frac{1}{\rho_0} \left\langle \theta \nabla_i p \right\rangle - \tau_{ij} \frac{\partial \left(\Theta + \overline{\Theta}\right)}{\partial x_j} - F_j \frac{\partial U_i}{\partial x_j} - \varepsilon_i^{(F)} ,$$

$$\tau_{ij} \equiv \left\langle u_i u_j \right\rangle = \delta_{ij} \frac{\left\langle \mathbf{u}^2 \right\rangle}{3} - K_M \left(\nabla_i U_j + \nabla_j U_i\right),$$

$$\varepsilon_K = \frac{E_K}{t_T}, \quad \varepsilon_i^{(F)} = \frac{F_i}{C_F t_T}, \quad \varepsilon_\theta = \frac{E_\theta}{C_P t_T},$$

CBL-Core for Shear-Free Convection

$$\frac{D\boldsymbol{\omega}}{Dt} = K_M \Delta \boldsymbol{\omega} - \beta\left(\mathbf{e}\times\nabla\right)\Theta + (\boldsymbol{\omega}\cdot\nabla)\,\mathbf{U}\,,$$

$$\frac{D\Theta}{Dt} = -\nabla\cdot\mathbf{F}\ ,$$

$$\boldsymbol{\omega} = \nabla \times \mathbf{U}$$

$$D/Dt = \partial/\partial t + U_k \partial / \partial x_k\ ,\quad \beta = g / T_0$$

$$\nabla\cdot\mathbf{F} = -t_T \sigma F_z^* \left(\mu \Delta_h - \Delta_z\right) U_z - K_H\, \Delta\Theta\,,$$

Solution for Cloud Cells (CBL-core)

$$U_r = -A_* U_{z0} J_1\left(\lambda \frac{r}{R}\right)\cos\left(\frac{\pi z}{L_z}\right),$$

$$U_z = U_{z0} J_0\left(\lambda \frac{r}{R}\right)\sin\left(\frac{\pi z}{L_z}\right),$$

$$\Theta = \Theta_0 J_0\left(\lambda \frac{r}{R}\right)\sin\left(\frac{\pi z}{L_z}\right),$$

$$\boldsymbol{\omega} = \mathbf{e}_\varphi \lambda \frac{U_{z0}}{R}\left(1 + A_*^2\right) J_1\left(\lambda \frac{r}{R}\right)\sin\left(\frac{\pi z}{L_z}\right).$$

$$A_* = \pi R / \lambda L_z$$

$$\frac{U_{z0}}{\Theta_0} = \frac{\beta L_z^2}{\pi^2 K_M} \frac{A_*^2}{\left(1 + A_*^2\right)^2},$$

$$\frac{K_M^2}{\beta F_z t_T R^2 \Pr_T} = \frac{\sigma}{\lambda^2} \frac{A_*^2 - \mu}{\left(1 + A_*^2\right)^3}.$$

EFB-Theory for CBL-Core for Shear-Free Convection

$$\frac{E_K}{E_U} = 3C_\tau A_z \left(\frac{l}{L_z}\right)^2 \frac{\Phi_1(A_*)}{1-\hat{F}},$$

$$\hat{F} \equiv \frac{\beta F_z t_T}{E_K} = \frac{(2\pi C_\tau A_z)^2}{\sigma \Pr_T} \frac{l^2}{L_z^2} \Phi_2(A_*),$$

$$\frac{E_\theta}{E_\Theta} = \frac{C_P C_F A_r}{7A_*^2}\left(\frac{l}{L_z}\right)^2,$$

$\langle \ldots \rangle_V$ implies the averaging over the volume of the semi-organized structure.

$$\frac{F_z}{\langle \Theta U_z \rangle_V} = \frac{1}{40}\left(\frac{l}{L_z}\right)^2.$$

$$U_D = \left[\left(F_z + \langle \Theta U_z \rangle_V\right)\beta L_z\right]^{1/3}$$

$$\Theta_D = \left(F_z + \langle \Theta U_z \rangle_V\right)/U_D$$

$$\frac{E_\Theta}{\Theta_D^2} = \frac{6C_P C_F C_\tau A_r A_z}{\left(1-\hat{F}\right)^{1/3}}\left(\frac{l}{L_z}\right)^{10/3}\left(1-\frac{F_z}{F_{\mathrm{tot}}}\right)^{4/3}\Phi_8(A_*),$$

EFB-Theory for CBL-Core for Shear-Free Convection

The kinetic energy of the semi-organized structures (cloud cells):

$$E_U \equiv \frac{1}{2} U_{z0}^2 = \frac{1}{3 C_\tau A_z} \left(\frac{L_z}{l} \right)^{4/3} \left(\langle \Theta U_z \rangle_V \beta L_z \right)^{2/3} \frac{\Phi_9(A_*)}{\Phi_1(A_*)} \left(1 - \hat{F}\right)^{1/3},$$

The thermal energy of the semi-organized structures (cloud cells):

$$E_\Theta \equiv \frac{1}{2} \Theta_0^2 = \frac{83}{2} \left(\frac{l}{L_z} \right)^{4/3} \left(\frac{\langle \Theta U_z \rangle_V^2}{\beta L_z} \right)^{2/3} C_\tau A_z \left(1 - \hat{F}\right)^{-1/3} A_*^2 \, \Phi_8(A_*).$$

$A_* = \pi R / \lambda L_z$

The mean vertical temperature gradient:

$$\frac{\partial \overline{\Theta}}{\partial z} = 12.7 \frac{\left(\langle \Theta U_z \rangle_V l \right)^{2/3}}{\beta^{1/3} L_z^2} \frac{C_F A_r}{A_z} \left(1 - \hat{F}\right)^{1/3} \Phi_6(A_*) \left[1 - \frac{A_z^2 \Pr_T \Phi_7(A_*)}{3 A_r \sigma (1 - \hat{F})} \right],$$

EFB-Theory for CBL-Core for Shear-Free Convection

The vertical flux of entropy transported by the semi-organized structures:

$$\langle \Theta U_z \rangle_V = \frac{1}{2} \Theta_0 U_{z0} J_2^2(\lambda) = (C_\tau A_z)^{3/2} \frac{l^2 U_{z0}^3}{\beta L_z^3} \frac{\Phi_4(A_*)}{(1-\hat{F})^{1/2}},$$

The ratio of fluxes of entropy :

$$\frac{\langle \Theta U_z \rangle_V}{F_z} = \frac{\sigma \Pr_T}{(C_\tau A_z)^2} \frac{L_z^2}{l^2} (1-\hat{F}) \Phi_5(A_*),$$

Production in Sheared Convection

The production of turbulence is caused by three sources:

a) the shear of the semi-organized structures:

$$\Pi^{(cs)} = -\left\langle \tau_{ij}\, \partial U_i / \partial x_j \right\rangle_V = K_M \left\langle S_{ij}\, S_{ji} \right\rangle_V$$

b) the background wind shear:

$$\Pi^{(s)} = K_M\, S^2$$

c) the buoyancy:

$$\hat{E}_K = E_K / L_y^2\, S^2 ,$$

$$\hat{E}_K \left(\frac{l}{L_y} \right)^2 >> 1 .$$

$$\frac{E_K}{E_U} = \frac{C_*}{4(1-\hat{F})} \left(\frac{l}{L_y} \right)^2 \left(\left(1 + A_*^2\right)^2 - 3\, A_*^2 \right) ,$$

$$C_* = 2\pi^2 C_\tau A_z ,$$

$$\frac{E_\theta}{E_\Theta} = \pi^2 C_P C_F\, A_z \left(\frac{l}{L_z} \right)^2 .$$

$$\frac{\left\langle \Theta U_z \right\rangle_V}{F_z} = \frac{\pi^2 \sigma \Pr_T}{4 C_*} \left(\frac{U_{z0}}{L_y\, S} \right)^2 \left(\frac{A_*^2 - \mu}{1 + A_*^2} \right) ,$$

Sheared Convection (CBL-core)

$$\frac{D\boldsymbol{\omega}}{Dt} = K_M \Delta\, \boldsymbol{\omega} - \beta(\mathbf{e}\times\nabla)\Theta + (\boldsymbol{\omega}\cdot\nabla)\,\mathbf{U} + (\boldsymbol{\omega}^{(s)}\cdot\nabla)\,\mathbf{U}\,,$$

$$\frac{D\Theta}{Dt} = -\nabla\cdot\mathbf{F}\ \ ,$$

$$\nabla\cdot\mathbf{F} = -t_T\left(\sigma F_z^*(\mu\Delta_h - \Delta_z)U_z + \frac{8}{15}\mathbf{F}_x^*\cdot(\mathbf{e}\times\nabla)\omega_z\right) - K_H\,\Delta\Theta\,,$$

The shear velocity:

$$\mathbf{U}^{(s)} = (Sz,0,0)$$

$$\boldsymbol{\omega}^{(s)} = (0,S,0)$$

$$A_* = L_y / L_z$$

The solution of linearized equations:

$$U_x = -U_{x0}\cos\left(\frac{\pi\, y}{L_y}\right)\sin\left(\frac{\pi\, z}{L_z}\right),$$

$$U_y = -A_* U_{z0}\sin\left(\frac{\pi\, y}{L_y}\right)\cos\left(\frac{\pi\, z}{L_z}\right),$$

$$U_z = U_{z0}\cos\left(\frac{\pi\, y}{L_y}\right)\sin\left(\frac{\pi\, z}{L_z}\right),$$

$$\Theta = \Theta_0\cos\left(\frac{\pi\, y}{L_y}\right)\sin\left(\frac{\pi\, z}{L_z}\right),$$

$$\frac{U_{x0}}{U_{z0}} = \frac{L_y^2\, S}{\pi^2 K_M}\left(1 + A_*^2\right)^{-1},$$

$$\frac{\Theta_0}{U_{z0}} = \frac{L_y^2\, S^2}{\pi^2 \beta K_M}\left(1 + A_*^2\right)^{-1}\left[1 + \frac{\pi^4 K_M^2}{L_y^4\, S^2}\left(1 + A_*^2\right)^2\right].$$

Budget Equations for Sheared Convection

$$\frac{DE_K}{Dt} + \nabla \cdot \mathbf{\Phi}_K = -\tau_{ij} \frac{\partial U_i}{\partial x_j} + \beta F_z - \varepsilon_K \,,$$

$$\frac{DE_\theta}{Dt} + \nabla \cdot \mathbf{\Phi}_\theta = -\left(\mathbf{F} \cdot \nabla\right)\Theta - F_z \frac{\partial \overline{\Theta}}{\partial z} - \varepsilon_\theta \,,$$

$$\frac{DF_i}{Dt} + \frac{\partial}{\partial x_j} \Phi_{ij}^{(F)} = \beta \delta_{i3} \left\langle \theta^2 \right\rangle - \frac{1}{\rho_0} \left\langle \theta \nabla_i \, p \right\rangle - \tau_{ij} \frac{\partial \left(\Theta + \overline{\Theta}\right)}{\partial x_j} - F_j \frac{\partial U_i}{\partial x_j} - \varepsilon_i^{(F)} \,,$$

$$\tau_{ij} \equiv \left\langle u_i \, u_j \right\rangle = \delta_{ij} \frac{\left\langle \mathbf{u}^2 \right\rangle}{3} - K_M \left(\nabla_i U_j + \nabla_j U_i\right),$$

$$\varepsilon_K = \frac{E_K}{t_T}, \quad \varepsilon_i^{(F)} = \frac{F_i}{C_F \, t_T}, \quad \varepsilon_\theta = \frac{E_\theta}{C_P \, t_T},$$

EFB-Theory for CBL-Core for Sheared Convection

The kinetic energy of the semi-organized structures (cloud streets):

$$E_U \equiv \frac{1}{2} U_{z0}^2 = \frac{2^{1/3}}{C_*} \left(\frac{L_y}{l} \right)^{4/3} U_D^2 \left(1 - \hat{F}\right)^{1/3} \Phi_{10}(A_*),$$

The thermal energy of the semi-organized structures (cloud streets):

$$E_\Theta \equiv \frac{1}{2} \Theta_0^2 = C_* \left(\frac{l}{2L_y} \right)^{4/3} \left(\frac{U_D^2}{\beta L_y} \right)^2 \left(1 - \hat{F}\right)^{-1/3} \Phi_{12}(A_*),$$

The Deardorff velocity scale:

$$U_D = \left(\langle \Theta U_z \rangle_V \beta L_z \right)^{1/3}$$

$$\hat{F} = \frac{C_*^2}{\pi^2 \sigma \, \mathrm{Pr}_T \, \hat{E}_K} \left(\frac{l}{L_y} \right)^2 \frac{\left(1 + A_*^2\right)^2}{(A_*^2 - \mu)},$$

The vertical turbulent flux of entropy:

$$F_z = \frac{2^{2/3} C_*^2}{\pi^2 \sigma \, \mathrm{Pr}_T} \left(\frac{l}{L_y} \right)^{4/3} \left(\frac{U_D L_y S^2}{\beta} \right) \left(1 - \hat{F}\right)^{-1/3} \Phi_{11}(A_*),$$

References (Stably Stratified Turbulence)

- **Zilitinkevich, S., Elperin, T., Kleeorin, N., and Rogachevskii, I, 2007:** Energy- and flux-budget (EFB) turbulence closure model for stably stratified flows. Boundary Layer Meteorology, Part 1: steady-state homogeneous regimes. *Boundary-Layer Meteorol., 125, 167-191.*

- **Zilitinkevich S., Elperin T., Kleeorin N., Rogachevskii I., Esau I., Mauritsen T. and Miles M., 2008:** Turbulence energetics in stably stratified geophysical flows: strong and weak mixing regimes. *Quarterly J. Royal Meteorol. Society,* 134, 793-799.

- **Zilitinkevich, S.S., Elperin, T., Kleeorin, V. L'vov, N., Rogachevskii, I., 2009:** Energy- and flux-budget turbulence closure model for stably stratified flows. Part II: the role of internal gravity waves. *Boundary-Layer Meteorol. 133*, 139-164.

- **Zilitinkevich, S.S., Elperin, T., Kleeorin, N., Rogachevskii, I., and Esau, I., 2013:** A hierarchy of energy- and flux-budget (EFB) turbulence closure models for stably stratified geophysical flows. Boundary-Layer Meteorol. 146, 341-373.

- **Eidelman A., Elperin T., Gluzman Y., Kleeorin N., and Rogachevskii I., 2013:** "Experimental study of temperature fluctuations in forced stably stratified turbulent flows". Phys. Fluids, 25, 015111.

- **Cohen N., Eidelman A., Elperin T., Kleeorin N., and Rogachevskii I., 2014:** "Sheared stably stratified turbulence and large-scale waves in a lid driven cavity". Phys. Fluids, 26, 105106.

- **Kleeorin N., Rogachevskii I., Soustova I. Troitskaya Yu., Ermakova O., Zilitinkevich S., 2019:** "Internal gravity waves in energy and flux budget turbulence-closure theory for shear-free stably stratified flows". Phys. Rev. E, 99, 063106.

References (Convective Turbulence)

- **Elperin T.**, **Kleeorin N.**, **Rogachevskii I.**, and **Zilitinkevich S.**, Formation of large-scale semi-organized structures in turbulent convection, *Phys. Rev. E* **66**, 066305 (1—15), (2002).
- **Elperin T.**, **Kleeorin N.**, **Rogachevskii I.**, and **Zilitinkevich S.**, Tangling turbulence and semi-organized structures in convective boundary layers, *Boundary-Layer Meteorol*., **119,** 449-472 (2006).
- **Elperin T.**, **Golubev I.**, **Kleeorin N.**, and **Rogachevskii I.**, Large-scale instabilities in turbulent convection, *Phys. Fluids,* ***18****, 126601 (1—11)*, (2006).
- **Bukai M., Eidelman A.**, **Elperin T.**, **Kleeorin N.**, **Rogachevskii I.**, **Sapir-Katiraie I.**, Effect of Large-Scale Coherent Structures on Turbulent Convection, *Phys. Rev. E* 79, 066302, (2009); "Transition Phenomena in Unstably Stratified Turbulent Flows". Phys. Rev. E, 83, 036302 (2011).
- **Rogachevskii I. and Kleeorin N., "Turbulent Fluxes of Entropy and Internal Energy in Temperature Stratified Flows". J. Plasma Phys., 81, 395810504 (2015).**
- **Zilitinkevich S., Kleeorin N.**, **Rogachevskii I.**, "EFB theory for Atmospheric Turbulent Convection: Surface Layers", in preparation.
- **Zilitinkevich S., Kleeorin N.**, **Rogachevskii I.**, "EFB theory for Atmospheric Turbulent Convection: CBL-Core", in preparation.

Conclusions

- Budget equations for the kinetic and potential energies and for the heat flux play a crucial role for analysis of stably stratified turbulence.
- Explanation for no critical Richardson number in stably stratified turbulence.
- Reasonable Ri-dependencies of the turbulent Prandtl number, the anisotropy of stably stratified turbulence, the normalized heat flux and TKE which follow from the developed theory.
- The scatter of observational, experimental, LES and DNS data in stably stratified turbulence are explained by effects of large-scale internal gravity waves on stably stratified turbulence.
- We have developed the energy and flux budget (EFB) turbulence theory that takes into account a two-way coupling between internal gravity waves (IGW) and the shear-free stably stratified turbulence produced by IGW. Due to the nonlinear effects more intensive IGW produce more strong turbulence. The low amplitude IGW produce turbulence consisting up to 90 % of turbulent potential energy.

Conclusions

- ❖ Predictions of energy- and flux-budget turbulence (EFB) theory are in a good agreement with the experimental results on stably stratified and convective turbulence, and with observations in atmospheric turbulence.

- ❖ In experiments with turbulent convection, we have found that there are many locations with stably stratified regions in the flow core of the large-scale circulation.

- ❖ In experiments with turbulent convection, we detect large-scale standing internal gravity waves excited in the regions with the stably stratified flow, and the spectrum of these waves contains several localized maxima.

THE END